Perspective

Molecular Models of Voltage Sensing

Chris S. Gandhi and Ehud Y. Isacoff

Department of Molecular and Cell Biology, University of California, Berkeley, CA 94720

Voltage-gated ion channels have always been overachievers. They have the singular distinction of having solved the permeation problem five times over. Not only do they have a central, highly selective pore through which they conduct charged ions, they also have four peripheral "pores" or gating canals through which they conduct the charged portions of their voltage sensors. This trick of protein permeation generates a small gating current as the S4 arginines and lysines move through the electric field of the membrane and ultimately results in channel opening.

The membrane-spanning portion of voltage-gated channels contains two classes of functional domains. Four voltage-sensing domains located at the periphery of the tetramer surround a central pore forming domain (Fig. 1 B). The pore domain of the voltage-gated K^+ (Kv) channels share structural homology with the bacterial KcsA and MthK channels whose crystal structures have been solved (Doyle et al., 1998; Jiang et al., 2002). The pore domain consists of S5, the P-loop, and S6 which constitute the ion permeation pathway, including the selectivity filter and two of the gates (Fig. 1). The voltage-sensing domains, whose crystal structures have yet to be determined, are the subject of this Perspective. The four positively charged S4s, located between S1-S3 and the pore domain, function as voltage sensors. Membrane depolarization drives the positively charged residues of S4 through the gating canal. The movement of these charges through the membrane electric field generates the gating current that precedes channel opening. Below, we explore possible models of voltage sensor structure and motion with the ultimate goal of understanding how voltage-sensor rearrangements drive the pore domain gates to open and close. We begin by outlining eight fundamental experimental observations in the field and then discuss models that could account for these observations.

The Data

(1) S4 contains a conserved three residue repeating sequence motif {+, X_1, X_2, +, X_1, X_2...}. The S4 sequence motif is conserved across a large super-family of voltage-gated channels. S4 contains a basic residue at every third position, followed by two hydrophobic residues in a sequence with 4–8 repeats. Movement of the basic resides generates the gating current. Additionally, the residues between the positive charges appear to play a distinct role. Scanning perturbation analysis of Kv2.1 and EAG has shown that S4 contains a high impact positive charge (+), followed by a high-impact hydrophobic residue (X_1) and a low-impact hydrophobic residue (X_2) (Figs. 2 A and 3 B; Li-Smerin et al., 2000a; Schönherr et al., 2002). High impact residues are thought to lie at a protein–protein interface, where their mutation can disrupt protein packing and thus impact gating. Low impact residues are thought to face lipid or water (see sections 3 and 4; Fig. 3 B and 4). Within the short length of the gating canal, the low impact residues would lie on one face of an α-helix and face lipid. The basis for thinking that S4 adopts a helical conformation is the perturbation analysis of Li-Smerin et al. (2000a) and the observation that synthetic S4 peptide form helices (Peled-Zehavi et al., 1996). The {+, X_1, X_2...} repeat paints three parallel left-handed spirals with a slow pitch along the length of a right-handed helical S4 (Fig. 3 B).

(2) Each subunit carries ~3 gating charges, contributed mainly by R1-R4 in S4. Wild-type Shaker channels displace ~3.2–3.4 charges per subunit as the channel gates from the resting to the activated state (Schoppa et al. 1992; Seoh et al., 1996; Aggarwal and MacKinnon, 1996). Neutralizations of the S2/S3 negative charges and S4-positive charges have identified the residues that carry the gating charge. Studies from the MacKinnon and Bezanilla labs showed that charge neutralizations reduce the gating charge and that S4 carries most of it (Aggarwal and MacKinnon, 1996; Seoh et al., 1996). In one study neutralization of R2, R3, R4, and K5 reduced the gating charge by 1.2, 1.7, 1.5, and 1.4 charges per subunit (Seoh et al., 1996); in the other study neutralization of R1, R2, R3, R4, and K5 reduced gating charge by ~1, ~1, ~1, ~1, and ~0.5 per subunit (Aggarwal and MacKinnon, 1996).[1] Both studies found a contribution for K5, the fifth charge, although the gating charge associated with this residue was reduced. In support of these observations, a histidine substituted for R2, R3, or R4 transports a proton across the membrane (Starace et al., 1997; Starace and Bezanilla 2001). This was not true at K5, indicating that K5 does not cross the electric field. Together, the three studies

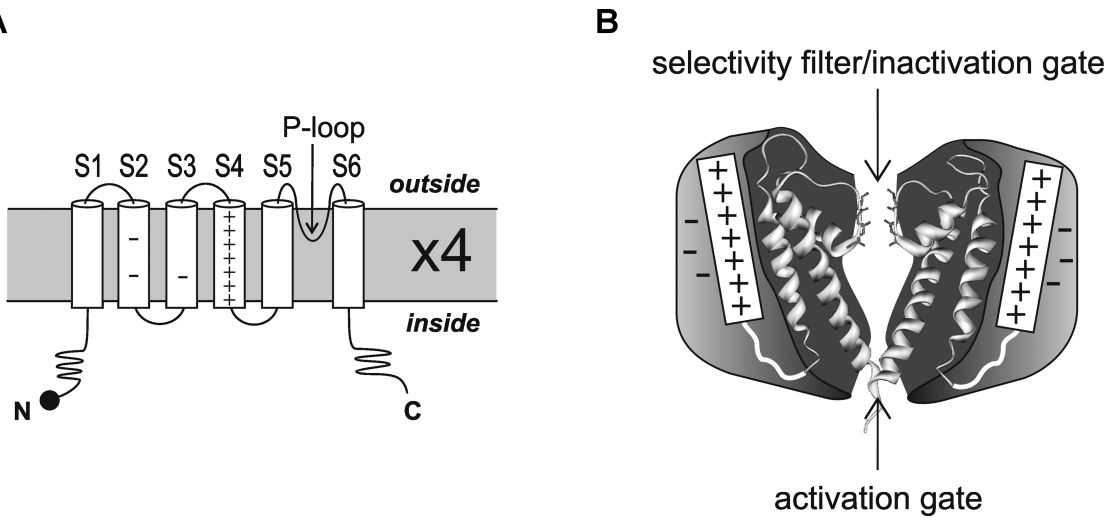

FIGURE 1. Voltage-gated ion channel structure. (A) Topology model of a single voltage-gated channel subunit. Each subunit has six transmembrane segments, S1–S6. S4 has a series of four to seven positive charges at every third position; S2 and S3 contain three conserved negative charges that interact electrostatically with S4; S5/P-loop/S6 form the pore domain which is homologous to the bacterial KcsA channel. (B) Cartoon of how voltage-sensing domains may wrap around a central KcsA-like pore domain. Two subunits are shown from the side.

lead to the conclusion that the majority of the gating charge is carried by R1-R4 (Fig. 2).

(3) S4 spans the membrane in 10 residues. Accessibility scanning of Shaker channels with thiol-reactive MTS reagents has shown that a sequence of ~10 residues is inaccessible to both the internal and external solution in the resting state (Figs. 2 B and 3 A; Larsson et al., 1996; Baker et al., 1998). A 10 residue sequence corresponds to 13.5 Å of axial length of an α-helix, a length considerably shorter than the thickness of the hydrophobic core of the membrane. This indicates that S4 resides in a short gating canal, with a deep watery vestibule on either one or both side(s) (Fig. 4). A 10 residue length can include a maximum of 4 positive charges; however, given the topology of S4, only 2 and 3 positive charges occupy the gating canal in the resting and activated states (Figs. 2 B and 4). Along the gradual pitch of the {+, X_1, X_2...} repeat, three neighboring positive charges would lie within 120° of each other, suggesting that they interact with one surface of the gating canal.

[1]The sum of the total gating charge reduction from each neutralization exceeds the ~3.3 gating charge per subunit of wild-type channels. Seoh et al. (1996) found a summed reduction of 5.8, even without the neutralization of R1. Aggarwal and MacKinnon (1996) obtained a value of 4.5. These excessive total values of charge reduction, along with the cases where single neutralizations reduced gating charge by more than the maximal possible value of 1 (the case for a charge that completely crosses the membrane), together suggest that each basic residue contributes to gating charge directly by moving through the electric field and indirectly by influencing the shape of the electric field or the position of the other charged side chains in the field. This indicates that the amount of charge carried by each residue was likely over-estimated in these studies.

(4) Activation moves S4 through the canal by nine residues. Fluorescence measurements show that membrane depolarization induces a rearrangement of S4 with the correct voltage dependence and kinetics to account for the transmembrane displacement of the gating charge (Mannuzzu et al., 1996; Cha and Bezanilla, 1997; Baker et al., 1998; Gandhi et al., 2000). Accessibility scanning shows that this process involves the motion of a nine residue sequence of S4 from an inaccessible location within the gating canal into the external solution (Larsson et al., 1996; Mannuzzu et al., 1996; Yusaf et al., 1996; Baker et al., 1998; Wang et al., 1999; Schönherr et al., 2002). At the same time, a sequence of ~9 residues disappears from internal exposure (Larsson et al., 1996; Baker et al., 1998). This indicates an outward activation motion of S4 relative to the gating canal. The motion exchanges virtually the entire buried portion of S4 (Fig. 3 A). An outward motion is in the correct direction to generate the gating charge. A similar motion takes place in Na^+ channels (Yang et al., 1996).

(5) S4 rotates during activation. The Bezanilla and Isacoff labs have measured fluorescence resonance energy transfer (FRET) between a donor probe and an acceptor probe attached to identical S4 residues on different subunits. Both groups observed a pattern of deduced distance changes that suggest a helical rotation of ~180° upon activation (Cha et al., 1999; Glauner et al., 1999). Despite agreement about the overall pattern of the distance change, there were differences between the studies concerning which residues moved closer and further apart. These discrepancies may have been due to differences in the pointing angle from the protein backbone between the La^{3+}-chelate donor (paired

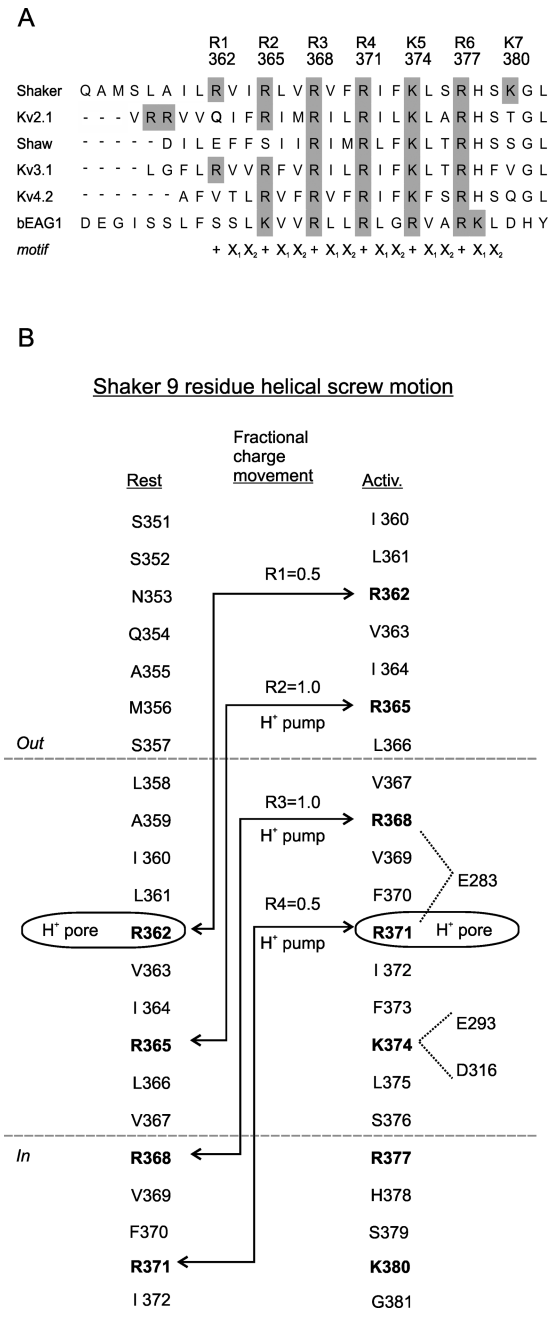

FIGURE 2. S4 sequence, gating charge, and proton transport for a S4 helical screw motion. (A) Alignment of S4s from Kv subfamilies. Shaker belongs to the Kv1 subfamily. Shaw belongs to Kv3. EAG is aligned to Shaker based on accessibility probing (see Fig. 3A). The register of the sequence repeat {+, X_1, X_2, +, X_1, X_2...} is shown below the alignment. (B) Topology of Shaker S4 in resting and activated states based on accessibility analysis. Charge displacement by R1 to R4 is calculated assuming a linear drop of the electric field over the length of the gating canal and assuming no change in canal shape. Note that positions where histidine transports protons across the membrane (H^+ pump) must at least reach the middle of the gating canal. A histidine at the middle turns the gating canal into a proton pore, suggesting the existence of a proton conduction pathway from both ends of the canal to the center. Electrostatic interactions of R3, R4, and K5 with negative residues E283 and E293 in S2 and D316 in S3 are shown for the activated state.

with a fluorescein acceptor) in the one study (Cha et al., 1999) and the fluorescein donor (paired with a tetramethylrhodamine acceptor) in the other study (Glauner et al., 1999). However, the voltage-dependent distance changes of both studies both support an activation motion that involves a rotation of S4.

(6) The voltage sensor has stable intermediate states. Two classes of evidence indicate intermediate voltage sensor states. First, two phases of gating charge movement can be easily resolved kinetically (Bezanilla et al., 1994). Second, two sequential outward motions of S4 accompany these gating charge movements, with an intermediate S4 transmembrane position between them (Baker et al., 1998). In addition, kinetic models of gating require multiple gating charge carrying steps in each subunit, with the most comprehensive model (the 3 + 2′ model) calling for three charge-carrying steps per subunit followed by two cooperative steps (Schoppa and Sigworth, 1998).

(7) The gating canal can form a proton pore. Replacement of either R1 or R4 with histidine allows the gating canal to conduct protons (Starace and Bezanilla, 1999, 2001). This suggests that the gating canal can accommodate a water pathway that provides a proton conduction path that can bridge the internal and external solutions by a single properly placed histidine. An arginine at the same position disrupts the proton conduction pathway. Proton pore formation occurs at two sites but in opposite states. R1H forms a proton pore in the resting state; R4H forms a proton pore in the activated state.

(8) S2/S3, the pore domain, and lipid likely form three "walls" of the gating canal. Interaction between three conserved negative residues in S2 and S3 and positive residues in S4 suggests that S2 and S3 line one side of the gating canal (Papazian et al., 1995; Seoh et al., 1996; Tiwari-Woodruff et al., 1997, 2000). This is compatible with a helix packing model based on perturbation analysis of S1-S4 (Li-Smerin et al., 2000a). The three negative residues in S2 and S3 match the maximum of three positively charged S4 residues that can occupy the canal at one time (section 3; Fig. 4).

Fluorescence and perturbation analysis suggest that the pore domain forms another side of the canal (Gandhi et al., 2000; Li-Smerin et al., 2000b; Loots and Isacoff, 2000). This is supported by the findings that the activation motion of S4 brings R1 and R2 into the proximity of residue E418 in the pore domain turret (Elinder et al., 2001) and that a cysteine introduced into S4 can cross-link with one introduced into the pore domain (Gandhi and Isacoff, 2002; Laine et al., 2002).

The S2/S3 and pore domain walls of the gating canal are believed to interact with the high impact sides of S4. The last side of the gating canal is presumed to be lipid, based on the hydrophobic nature of the X_2 posi-

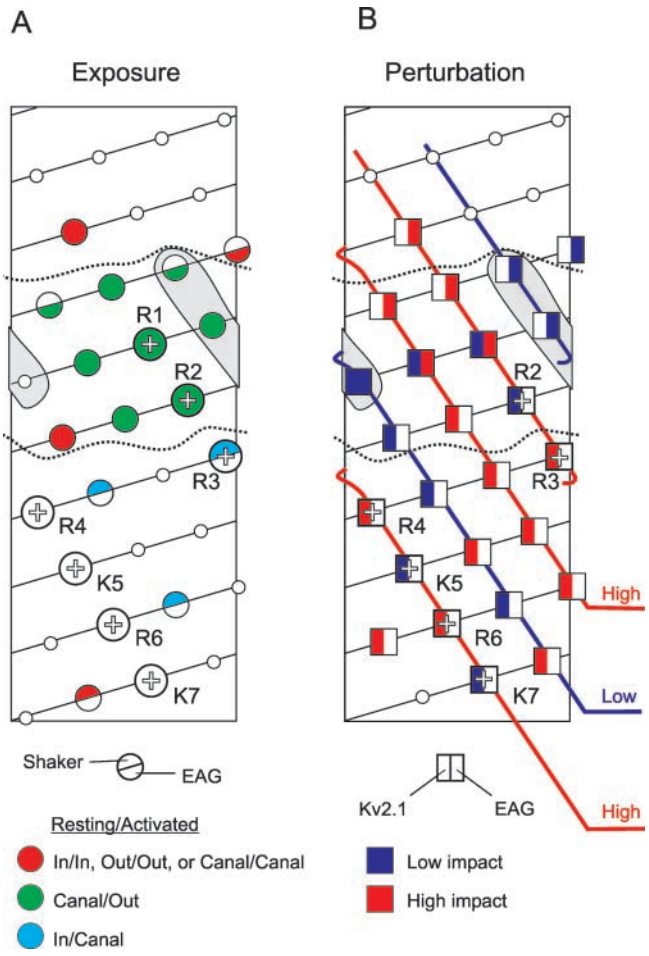

FIGURE 3. S4 accessibility and perturbation analyses. (A) Helical net model of S4 resting state topology in bEAG1 and Shaker (external end up, starting at bEAG1 site 312 and Shaker site 350) based on accessibility of bEAG1 and Shaker. Dotted lines indicate external and internal boundaries of the gating canal in the resting state. Note that R1 is absent in EAG. (B) Perturbation of slow gating mode by cysteine mutations in bEAG1 and of the conductance-voltage relation by alanine mutations in Kv2.1. EAG high-impact sites are in the canal at rest consistent with mode switching in the resting state. Kv2.1 high impact sites are in the canal in the activated state consistent with the activated state having the greatest impact on opening. Three parallel stripes along S4 (high-impact charged stripe, high-impact hydrophobic stripe and low-impact hydrophobic stripe) are continuous between bEAG1 and Kv2.1, forming three threads of a helical screw. Note that both EAG and Kv2.1 are missing R1 (see Fig. 2 A).

tion of S4 and because mutations of those residues have a low impact on gating (Li-Smerin et al., 2000a; Schönherr et al., 2002).

The Synthesis

Axial translation of S4 relative to the gating canal: R1-R4 carry the gating charge. In an attempt to synthesize the above observations, we first ask whether S4s exposure change (sections 3 and 4) can account for the gating charge (section 2). Assuming a constant electric field, we can predict the contribution to the gating charge from each of S4's basic residues during the nine residue outward exposure change of activation. In Shaker, R1 moves from the middle of the gating canal to the external solution. R2 moves from the internal end of the canal to the external solution. R3 moves from the internal solution to the outer end of the gating canal, and R4 moves from the internal solution into the middle of the gating canal (Fig. 2 B). This predicts that R1-R4 alone carry ~0.5, 1.0, 1.0, and 0.5 gating charges, respectively, for a total of three per subunit. The predicted total is close to the measurements in wild-type channels of 3.2–3.4 charges (Schoppa et al., 1992; Aggarwal and MacKinnon, 1996; Seoh et al., 1996). Taking into account that charge neutralizations over-estimate the contribution of each basic residue (footnote to section 2), the predicted values reasonably approximate the experimental data (see section 2).

A Nine Residue Helical Screw Motion in Three Ratchet Steps

Below we describe how a model of S4 motion predicted by S4's sequence motif (section 1) and exposure change (section 4) accounts for four very different experimental observations (sections 5–8). Each of the three parallel left-handed spirals of the {+, X_1, X_2...} repeat (Fig. 3 B) is predicted to face a particular wall of the gating canal. The positive residues should face S2/S3 so that they can interact with negative countercharges. The X_2 low impact hydrophobic residues should face lipid, and the high impact hydrophobic X_1 residues should pack against the remaining protein surface of the pore domain (see section 8). To maintain these interactions, an axial translation of the S4 relative to the gating canal would require either a rotation of S4 to the left (clockwise, as seen looking down onto the membrane from the outside) (Fig. 4) or a rotation of the gating canal to the right (counter-clockwise, as seen from the outside). Following the helical screw model of S4 motion proposed originally by Guy and Seetharamulu (1986) and Catterall (1986), we have added two additional "threads" (X_1 and X_2) to the positively charged thread. Based on accessibility analysis we have considerably shortened the length of S4 buried in the gating canal. We also consider that rearrangements of the canal may be partly responsible for S4's exposure change. Coupling axial translation with rotation provides a low energy molecular pathway through the gating canal for the S4 side chains (Lecar and Larsson, 1997).

There are four pieces of evidence consistent with the helical screw model: (a) 180° rotation. A nine residue axial translation of S4 along the pitch of S4's threads produces a 180° rotation (Fig. 4). This agrees remarkably with the conclusions of the FRET studies, which arrived at a 180° rotation (section 5). There is agreement with the magnitude of the rotation and the identity of

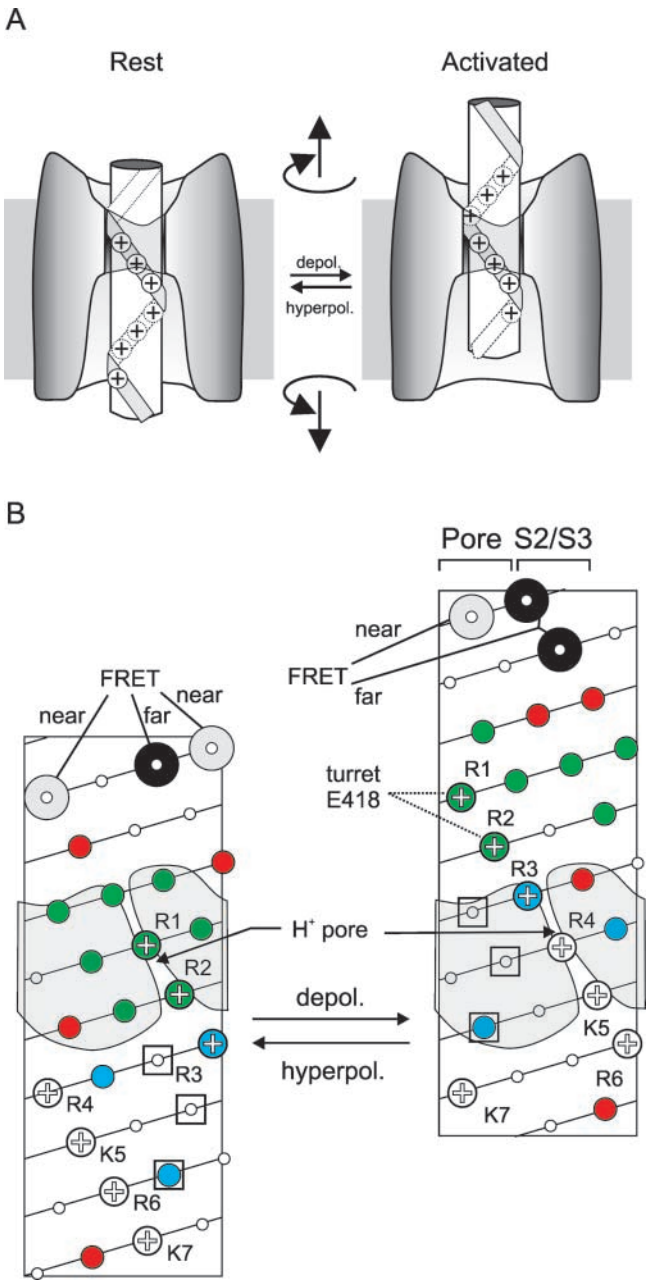

FIGURE 4. Helical screw motion accounts for S4 rotation, electrostatic interaction with the turret, and proton transport. (A) Cartoon of one version of a helical screw motion depicting S4 moving through an immobile canal. (B) S4 topology in resting state (left) and activated state (right) depicting S4 rotating and making an axial translation. (Note that axial translation of canal is equally viable.) Residues are color coded as in Fig. 3 A, except that data on Shaker and EAG is combined. The location of S2/S3 is placed to interact with S4's positive charges in the gating canal. The pore domain is placed to interact with the high impact hydrophobic stripe (see Fig. 3 B). This placement agrees with the Glauner et al. (1999) FRET study, which found that the residues predicted by the helical screw motion to face the pore in the activated state lie closest to the central axis, whereas residues found by FRET to lie furthest from the central are predicted by the helical screw motion to face S2/S3. The helical screw motion also predicts R1 and R2 to face the pore domain in the activated state and explains their electrostatic interaction in that state with E418. Note also that the ILT residues (three open squares), shown by Ledwell and Aldrich (1999) to influence coupling between activation and opening, are predicted by the helical screw model to all enter the canal only in the activated state and interact with the pore domain.

the residues that face the pore in each state. The residues predicted to face the pore domain in the activated state by the helical screw model were found in our FRET study to point toward the pore (Glauner et al., 1999), whereas residues predicted to face S2/S3 are deduced by FRET to point away from the pore domain (Fig. 4), supporting the model.

(b) Ratchet steps via semistable intermediates. The helical screw model predicts that the screw motion may stop at stable intermediate positions during activation as each basic charge ratchets into the position formerly occupied by the charge ahead of it. A nine residue axial translation of a pure helical screw produces three ratchet steps with two intermediate stopping points. Each ratchet step carries 1/3 of the total gating charge per subunit, i.e., one charge (Figs. 2 B and 4). An electrostatic model based on this idea accounts well for the steady-state voltage dependence of the gating charge in wild-type channels and in channels with neutralization mutations in S4 (Lecar and Larsson, 1997). This structural prediction is consistent with the 3 + 2′ model of Schoppa and Sigworth (1998), in which activation also occurs in three sequential charge carrying steps in each subunit. However, in the 3 + 2′ model the steps displace more gating charge in the first step, moving, sequentially, 1.0, 0.6, and 0.6 charges per subunit in the first three independent steps and a total of 1.8 charges per channel (all four subunits) in the last two cooperative steps. These values are likely an underestimate, since the total charge of the model accounts for only 75% of the measured charge.

Experimental data also indicate the existence of intermediate positions. Gating current measurements detect two prominent phases of gating charge motion (section 6). Moreover, a mutation that stabilizes the gating charge intermediate stabilizes S4 in an intermediate topology (Baker et al., 1998). Together, these findings show that S4 stops at least at one intermediate point as it moves its charges across the gating canal. But why is only one kinetic intermediate readily observed in wild-type channels? Perhaps the ratchet steps are not equivalent and one of the intermediates is more stable than the other. Such a difference could be due to variations in how particular amino acid side chains of S4 pack in the canal. It may also point to the existence of an additional conformational rearrangement, which could explain why the first step of the 3 + 2′ model car-

ries more charge. We consider the latter possibility in the final section of this Perspective.

(c) Turning the gating canal into a proton pore. Another piece of evidence explained by the helical screw model is the finding that histidine substitution at two S4 arginines turn the gating canal into a proton pore. R1H turns the gating canal into a proton pore in the resting state, and R4H does so in the activated state (Starace and Bezanilla, 1999, 2001). What does R1H in the resting state have in common with R4H in the activated state? The helical screw model predicts that in these opposite states they occupy the same location in the middle of the gating canal (Figs. 2 B and 4). If correct, this would imply that a water pathway for proton conduction exists from the internal solution to the external solution on the charged (S2/S3) side of the canal – a plausible expectation given the charged nature of this environment – and that this pathway is disrupted when an arginine is located in the middle of the canal. However, when histidine replaces arginine there is either enough room to form a continuous water wire along that face of the canal, or the histidine provides a bridge between internal and external water wires. It is not surprising that protons can penetrate deep into a crevice that was not detected by the thiol reagents used to determine the gating canal boundaries (sections 3 and 4; Fig. 3 A), since protons can conduct along a water wire of ≤2 Å (Pomes and Roux, 2002), whereas the thiol reagents used were 6 Å or greater in size.

(d) Electrostatic interaction between R1/R2 and E418 in turret. The helical screw motion of activation predicts R1 and R2 to move from the canal at rest, where they face S2/S3, into the external solution to face the pore domain (Fig. 4). This is consistent with R1 and R2 having electrostatic interaction with turret residue E418, but only in the activated state (Elinder et al., 2001).

An additional attraction of the helical screw model is that it provides a possible structural explanation for the behavior of mutants that disrupt coupling between activation and opening. Three such mutations in S4 ("ILT") studied by Ledwell and Aldrich (1999) are predicted by the helical screw model to fully enter the gating canal only in the activated state and to interact with the pore domain (Fig. 4).

The Helical Screw Compared with a Rotation in Place

The observations described above are all compatible with a helical screw motion. They are not compatible with a simple S4 rotation since this would have predicted a swap between internally and externally accessible faces of S4. For example, during activation positions R1 and R2 move from an inaccessible position in the gating canal to the external solution. A simple rotation would predict that the intervening positions on the opposite face of the helix would demonstrate the reverse change in accessibility. However, what is measured instead is an exposure upon activation of a continuous segment representing almost three helical turns of S4 (Fig. 3 A; Larsson et al., 1996; Yusaf et al., 1996; Baker et al., 1998; Wang et al., 1999; Schönherr et al., 2002; also see Horn, 2002, this issue). In addition, a rotation from an internal water-filled crevice to an external one provides no obvious basis for the observed early and late phases of the gating current, while the helical screw provides intermediate stopping points at each ratchet step.

The helical screw motion could work in two ways. The original model conceived by Guy and Seetharamulu (1986) and Catterall (1986) moves S4 through a fixed gating canal. S4 undergoes an outward axial translation accompanied by a left-handed rotation along the charged thread. In this case S4 acts as a screw turning through an immobile bolt formed by the gating canal. A plausible alternative is that a rotation occurs in S4 but part or all of the translation occurs in the canal. This would be akin to turning the screw in place and having the bolt slide down. Alternatively, the activation rearrangement may look nothing like a screw and bolt, even if it is driven by the S4–canal interactions that we have discussed for the helical screw model. Rearrangements of the other transmembrane segments around S4 may produce the same S4 exposure change. The actual activation rearrangement may involve a reorientation of S2 and S3 that opens access to the external end of S4 while closing access to the internal end of S4. To distinguish between these models, one would need to determine whether S4 or the canal undergoes an axial translation relative to an immobile reference, perhaps the membrane, and measure state-dependent accessibility changes of S2, S3, and the outer surface of the pore domain.

Does S4 Undergo an Axial Translation?

Three commendable efforts have been made to detect S4 axial translation or to determine the impact of constraining such motion, but they have not led to a conclusive answer. Cha et al. (1999) used FRET to measure voltage dependent distance changes between identical sites in different subunits at a site approximately midway in the S3-S4 linker. They found that the distance-voltage relation rose monotonically with depolarization and followed closely the charge-voltage relation. This observation does not support a pure outward translation perpendicular to the membrane (i.e., with no rotation), since the distance would be expected to be the same when all subunits are either resting ("in") or activated ("out") and maximal at the midpoint of the charge-voltage relation where some S4s are at rest and others are activated. However, for several reasons this

observation does not rule out outward translation. First, as one moves a reporter probe further away from S4 and into the S3-S4 linker, any outward translation of S4 should be lessened since at some point the linker must turn back toward the membrane. Second, even in the absence of an axial translation, a helical rotation of S4 predicts that the distance between the tested positions is greatest when all of the subunits are either in the resting or activated state. The proper test of translation, therefore, is not for pure translation, but for translation accompanied by rotation. In this case the distance would increase with voltage without hitting a maximum at the midpoint of the charge-voltage relation, but simply rise more sharply than the charge-voltage relation. Indeed, a tendency of this kind was observed (Cha et al., 1999). A third weakness of the argument is that if S4 lies at a tilted angle, as has been proposed (Tiwari Woodruff et al., 1997; Glauner et al., 1999; Li-Smerin et al., 2000b), then, depending on the tilt angle, even a pure axial translation might produce little or no distance maximum at the mid-point of the charge voltage relation.

An alternative approach to the question, such as transmembrane FRET between GFP near the internal end of S6 and tetramethylrhodamine maleimide at the outer end of S4 (Starace and Bezanilla, 2002), encounters the same problem described above if S4 is tilted. There are also two additional complications. First, gating motions are thought to occur at the internal end of S6 (Yellen, 1998; Jiang et al., 2002). Such motions are large enough to change the fluorescence of GFP attached 20 residues after the internal end of S6 in Shaker (Siegel and Isacoff, 1997; Guerrero et al., 2002). This means that the GFP may not act as an immobile reference to measure the motion of S4. Second, the transmembrane distance is much greater than R_0, so that one is in a flat part of FRET efficiency-distance relation, where even large changes in distance cannot be measured accurately.

Another argument against outward translation came from a study that found that deletion of the entire S3-S4 linker in Shaker does not prevent activation (Gonzalez et al., 2000). This seems incompatible with the idea of an axial S4 translation, regardless of tilt angle. However, one does not know what happens to the transmembrane segments when a linker is deleted, and it is possible that the outer end of S3 (S3C) unwinds to form a substitute linker. Arguing against this was the finding that for linkers less than six residues in length, sequentially adding back residues to the deletion yielded a periodic impact on the conductance-voltage relation, consistent with an α-helix (Gonzalez et al., 2001). At first glance, this seems like a good argument for S4 rotation without translation, since a half turn would be a motion of ~5 Å of the α-carbon and this is not that different from the 7.5 Å axial length of a six residue α-helix. However, to be readily interpreted, the determining factor in the impact of linker length on gating should be the length and not the amino acid sequence. Unfortunately, when other minimal linkers of less than six residues were used, with different amino acid identities, the impact pattern was very different and the periodic dependence of perturbation on length was lost even though the sequences seemed likely to have a similar helical propensity. It therefore seems that sequence is more important than length, an intriguing finding, but one that does not lead to a ready conclusion about the type or magnitude of S4's motion.

Rearrangement of the Gating Canal

We have obtained evidence for one kind of canal rearrangement in the EAG Kv channel (Schönherr et al., 2002). EAG channels switch from a fast to slow gating mode at negative voltage in the presence of external Mg^{2+}. We found that switching to the slow gating mode occurs due to a slowing of S4's outward motion. The molecular mechanism appears to be as follows. Accessibility analysis indicates that the sequence of EAG's S4 that occupies the gating canal at rest has ~30% smaller side chain volume than the sequence which resides in the canal in the activated state. Moreover, EAG lacks R1 (Fig. 2 A), so S4 motion changes the positive charge occupancy of the canal from one in the resting state to three in the activated state (see Figs. 2 B and 4). The combination of the change in charge occupancy and side chain volume requires a change in canal conformation, especially in the first two activation ratchet steps. We hypothesize that activation of S4 causes the gating canal to widen in order to accommodate the change in side chain volume. Fluorescence measurements support the prediction of canal rearrangements and show that an S4 probe that faces the protein walls of the canal, but not the lipid wall, senses the mode switching rearrangement. This indicates that mode switching is due to a motion of the canal, rather than of S4. A specialized feature of EAG allows Mg^{2+} coordination between EAG-specific acidic residues in S2 and S3 to stabilize the narrow canal conformation, and thus to trap S4 in its resting state (Silverman et al., 2000). We think that cross-bridging of S2 and S3 via Mg^{2+} holds the gating canal in the narrow conformation, and that for S4 to activate Mg^{2+} must first dissociate, permitting the canal to widen.

Other Kv channels are not predicted to have as dramatic a change in the character of canal occupancy as a result of activation (Fig. 2), and so would not need large rearrangements of the canal. In Shaker, S4-positive charge occupancy and volume change occur only in the first ratchet step (Figs. 2 and 3A). If this drove a

canal rearrangement it could explain the larger gating charge associated with the first of the three subunit steps of the Schoppa and Sigworth (1998) model. This could also account for the detection of an early phase of gating charge motion by fluorescence just outside S2 (Cha and Bezanilla, 1997). It remains to be seen whether specialized gating canal motions in early ratchet steps alter S4 exposure.

Conclusion

Similar to the short (∼12 Å) and narrow ion selectivity filter, which is open to water at either end, the short (∼13.5 Å) gating canal has water-filled vestibules at its ends. The short length of the canal focuses the electric field on a small sequence of S4, minimizing the contact surface and the number of charges placed in the low dielectric environment, while still providing a large gating charge. The full activation rearrangement is predicted to carry the helical screw through three ratchet steps, with each step moving an S4 charge into the position of the one ahead of it and carrying a charge of ∼1, for a total gating charge of ∼3. This helical screw motion—a 180° rotation plus 9 residue (13.5Å) axial translation—may occur entirely in S4 or alternately S4 may rotate while the equivalent of an axial translation occurs as a result of a rearrangement of the gating canal. Further studies will be needed to resolve this issue. More relevant to channel function will be to define the motion of S4 with respect to the pore domain, since it is this rearrangement that in a still unknown way controls the gating state of the pore.

We would like to thank Lidia Mannuzzu, Medha Pathak, Arnd Pralle, and Camin "Blondie" Dean for helpful comments on the manuscript and for valuable discussion.

REFERENCES

Aggarwal, S.K., and R. MacKinnon. 1996. Contribution of the S4 segment to gating charge in the Shaker K+ channel. *Neuron*. 16: 1169–1177.

Baker, O.S., H.P. Larsson, L.M. Mannuzzu, and E.Y. Isacoff. 1998. Three transmembrane conformations and sequence-dependent displacement of the S4 domain in shaker K+ channel gating. *Neuron*. 20:1283–1294.

Bezanilla, F., E. Perozo, and E. Stefani. 1994. Gating of Shaker K+ channels: II. The components of gating currents and a model of channel activation. *Biophys. J.* 66:1011–1021.

Catterall, W.A. 1986. Molecular properties of voltage-sensitive sodium channels. *Annu. Rev. Biochem.* 55:953–985.

Cha, A., and F. Bezanilla. 1997. Characterizing voltage-dependent conformational changes in the Shaker K+ channel with fluorescence. *Neuron*. 19:1127–1140.

Cha, A., G.E. Snyder, P.R. Selvin, and F. Bezanilla. 1999. Atomic scale movement of the voltage-sensing region in a potassium channel measured via spectroscopy. *Nature*. 402:809–813.

Doyle, D.A., J. Morais Cabral, R.A. Pfuetzner, A. Kuo, J.M. Gulbis, S.L. Cohen, B.T. Chait, and R. MacKinnon. 1998. The structure of the potassium channel: molecular basis of K+ conduction and selectivity. *Science*. 280:69–77.

Elinder, F., R. Mannikko, and H.P. Larsson. 2001. S4 charges move close to residues in the pore domain during activation in a K channel. *J. Gen. Physiol.* 118:1–10.

Gandhi, C.S., E. Loots, and E.Y. Isacoff. 2000. Reconstructing voltage sensor-pore interaction from a fluorescence scan of a voltage-gated K+ channel. *Neuron*. 27:585–595.

Gandhi, C.S., and E.Y. Isacoff. 2002. Optical measurements from a voltage-gated channel reveal interactions between voltage-sensing and opening. *Biophys. J.* 82:232a.

Glauner, K.S., L.M. Mannuzzu, C.S. Gandhi, and E.Y. Isacoff. 1999. Spectroscopic mapping of voltage sensor movement in the Shaker potassium channel. *Nature*. 402:813–817.

Gonzalez, C., E. Rosenman, F. Bezanilla, O. Alvarez, and R. Latorre. 2000. Modulation of the Shaker K(+) channel gating kinetics by the S3-S4 linker. *J. Gen. Physiol.* 115:193–208.

Gonzalez, C., E. Rosenman, F. Bezanilla, O. Alvarez, and R. Latorre. 2001. Periodic perturbations in Shaker K+ channel gating kinetics by deletions in the S3-S4 linker. *Proc. Natl. Acad. Sci. USA*. 98: 9617–9623.

Guerrero, G., M.S. Siegel, B. Roska, E. Loots, and E.Y. Isacoff. 2002. Tuning FlaSh: redesign of the dynamics, voltage range and color of the genetically-encoded optical sensor of membrane potential. *Biophys. J.* In press.

Guy, H.R., and P. Seetharamulu. 1986. Molecular model of the action potential sodium channel. *Proc. Natl. Acad. Sci. USA*. 83:508–512.

Horn, R. 2002. Coupled movements in voltage-gated ion channels. *J. Gen. Physiol.* 120:449–453.

Jiang, Y., A. Lee, J. Chen, M. Cadene, B.T. Chait, and R. MacKinnon. 2002. The open pore conformation of potassium channels. *Nature*. 417:523–526.

Laine, M., J.P.A. Bannister, W.R. Silverman, M.C. Lin, A.F. Mock, and D.M. Papazian. 2002. Structural interaction between voltage sensor and pore in Shaker K+ channels. *Biophys. J.* 82:231a.

Larsson, H.P., O.S. Baker, D.S. Dhillon, and E.Y. Isacoff. 1996. Transmembrane movement of the shaker K+ channel S4. *Neuron*. 16:387–397.

Lecar, H., and H.P. Larsson. 1997. Theory of S4 motion in voltage-gated channels. *Biophys. J.* 72:341a.

Ledwell, J.L., and R.W. Aldrich. 1999. Mutations in the S4 region isolate the final voltage-dependent cooperative step in potassium channel activation. *J. Gen. Physiol.* 113:389–414.

Li-Smerin, Y., D.H. Hackos, and K.J. Swartz. 2000a. alpha-helical structural elements within the voltage-sensing domains of a K(+) channel. *J. Gen. Physiol.* 115:33–50.

Li-Smerin, Y., D.H. Hackos, and K.J. Swartz. 2000b. A localized interaction surface for voltage-sensing domains on the pore domain of a K+ channel. *Neuron*. 25:411–423.

Loots, E., and E.Y. Isacoff. 2000. Molecular coupling of S4 to a K(+) channel's slow inactivation gate. *J. Gen. Physiol.* 116:623–636.

Mannuzzu, L.M., M.M. Moronne, and E.Y. Isacoff. 1996. Direct physical measure of conformational rearrangement underlying potassium channel gating. *Science*. 271:213–216.

Papazian, D.M., X.M. Shao, S.A. Seoh, A.F. Mock, Y. Huang, and D.H. Wainstock. 1995. Electrostatic interactions of S4 voltage sensor in Shaker K+ channel. *Neuron*. 14:1293–1301.

Peled-Zehavi, H., I.T. Arkin, D.M. Engelman, and Y. Shai. 1996. Coassembly of synthetic segments of shaker K+ channel within phospholipid membranes. *Biochemistry*. 35:6828–6838.

Pomes, R., and B. Roux. 2002. Molecular mechanism of h(+) conduction in the single-file water chain of the gramicidin channel. *Biophys. J.* 82:2304–2316.

Schoppa, N.E., K. McCormack, M.A. Tanouye, and F.J. Sigworth. 1992. The size of gating charge in wild-type and mutant Shaker

potassium channels. *Science*. 255:1712–1715.

Schönherr, R., L.M. Mannuzzu, E.Y. Isacoff, and S.H. Heinemann. 2002. Conformational switch between slow and fast gating modes: allosteric regulation of voltage sensor mobility in the EAG K^+ channel. *Neuron*. In press.

Schoppa, N.E., and F.J. Sigworth. 1998. Activation of Shaker potassium channels. III. An activation gating model for wild-type and V2 mutant channels. *J. Gen. Physiol.* 111:313–342.

Seoh, S.A., D. Sigg, D.M. Papazian, and F. Bezanilla. 1996. Voltage-sensing residues in the S2 and S4 segments of the Shaker K+ channel. *Neuron*. 16:1159–1167.

Siegel, M.S., and E.Y. Isacoff. 1997. A genetically encoded optical probe of membrane voltage. *Neuron*. 19:735–741.

Silverman, W.R., C.Y. Tang, A.F. Mock, K.B. Huh, and D.M. Papazian. 2000. Mg(2+) modulates voltage-dependent activation in ether-a-go-go potassium channels by binding between transmembrane segments S2 and S3. *J. Gen. Physiol.* 116:663–678.

Starace, D.M., and F. Bezanilla. 2002. Resonance energy transfer measurements of transmembrane motion in the Shaker K+ channel voltage sensing region. *Biophys. J.* 82:174a.

Starace, D.M., and F. Bezanilla. 2001. Histidine scanning mutagenesis of basic residues of the S4 segment of the shaker k+ channel. *J. Gen. Physiol.* 117:469–490.

Starace, D.M., and F. Bezanilla. 1999. Histidine at position 362 causes inwardly rectifying H+ conductance in the Shaker K+ channel. *Biophys. J.* 74:254a.

Starace, D.M., E. Stefani, and F. Bezanilla. 1997. Voltage-dependent proton transport by the voltage sensor of the Shaker K+ channel. *Neuron*. 19:1319–1327.

Tiwari-Woodruff, S.K., C.T. Schulteis, A.F. Mock, and D.M. Papazian. 1997. Electrostatic interactions between transmembrane segments mediate folding of Shaker K+ channel subunits. *Biophys. J.* 72:1489–1500.

Tiwari-Woodruff, S.K., M.A. Lin, C.T. Schulteis, and D.M. Papazian. 2000. Voltage-dependent structural interactions in the Shaker K(+) channel. *J. Gen. Physiol.* 115:123–138.

Wang, M.H., S.P. Yusaf, D.J. Elliott, D. Wray, and A. Sivaprasadarao. 1999. Effect of cysteine substitutions on the topology of the S4 segment of the Shaker potassium channel: implications for molecular models of gating. *J. Physiol.* 521:315–326.

Yang, N., A.L. George, and R. Horn. 1996. Molecular basis of charge movement in voltage-gated sodium channels. *Neuron*. 16: 113–122.

Yusaf, S.P., D. Wray, and A. Sivaprasadarao. 1996. Measurement of the movement of the S4 segment during the activation of a voltage-gated potassium channel. *Pflugers Arch.* 433:91–97.

Yellen, G. 1998. The moving parts of voltage-gated ion channels. *Q. Rev. Biophys.* 31:239–295.